Author Manuscript

Author Manuscript

Author Manuscript

Author Manuscript

HHS Public Access

Author manuscript

Dev Neurobiol. Author manuscript; available in PMC 2015 June 24.

Published in final edited form as:

Dev Neurobiol. 2009 June ; 69(7): 415–436. doi:10.1002/dneu.20717.

Adult neurogenesis in the crayfish brain: proliferation, migration and possible origin of precursor cells

Y. Zhang[1], **S. Allodi**[2], **D.C. Sandeman**[1], and **B.S. Beltz**[1,*]

Y. Zhang: yzhang3@wellesley.edu; S. Allodi: sallodi@histo.ufrj.br; D.C. Sandeman: dsandema@wellesley.edu; B.S. Beltz: bbeltz@wellesley.edu

[1]Neurobiology Program, Wellesley College, Wellesley, MA 02481

[2]Programa de Pós-Graduação em Ciências Morfológicas, ICB, Universidade Federal do Rio de Janeiro, Rio de Janeiro, Brazil

Abstract

The birth of new neurons and their incorporation into functional circuits in the adult brain is a characteristic of many vertebrate and invertebrate organisms, including decapod crustaceans. Precursor cells maintaining life-long proliferation in the brains of crayfish (*Procambarus clarkii*, *Cherax destructor*) and clawed lobsters (*Homarus americanus*) reside within a specialized niche on the ventral surface of the brain; their daughters migrate to two proliferation zones along a stream formed by processes of the niche precursors. Here they divide again, finally producing interneurons in the olfactory pathway. The present studies in *P. clarkii* explore (1) differential proliferative activity among the niche precursor cells with growth and aging, (2) morphological characteristics of cells in the niche and migratory streams, and (3) aspects of the cell cycle in this lineage. Morphologically symmetrical divisions of neuronal precursor cells were observed in the niche near where the migratory streams emerge, as well as in the streams and proliferation zones. The nuclei of migrating cells elongate and undergo shape changes consistent with nucleokinetic movement. LIS1, a highly conserved dynein-binding protein, is expressed in cells in the migratory stream and neurogenic niche, implicating this protein in the translocation of crustacean brain neuronal precursor cells. Symmetrical divisions of the niche precursors and migration of both daughters raised the question of how the niche precursor pool is replenished. We present here preliminary evidence for an association between vascular cells and the niche precursors, which may relate to the life-long growth and maintenance of the crustacean neurogenic niche.

Keywords

cell division; niche; LIS1; nucleokinesis; blood

Introduction

Many vertebrate and invertebrate organisms, including humans, retain the ability to make new neurons throughout life and to incorporate these into circuits in the adult brain. Adult-

*Mailing address: Neurobiology Program, Wellesley College, 106 Central Street, Wellesley, MA 02481, Telephone: 781-283-3048, FAX: 781-283-3642.

Author Manuscript Author Manuscript Author Manuscript Author Manuscript

born neurons in the crustacean brain differentiate into olfactory interneurons (Schmidt, 1997; Sullivan and Beltz, 2005), as do those in mammals (Gheusi and Lledo, 2007) and fish (Kaslin et al., 2008). The lineage of cells producing adult-born neurons in crayfish and clawed lobsters has been identified, is accessible on the ventral surface of the brain, and can be maintained in short-term culture (Sullivan et al., 2007a, b; Benton and Beltz, 2008). The goal of our present work was to examine in detail the proliferation and migration of neuronal precursor cells in this system.

In the brains of adult decapod crustaceans, cells continue to proliferate in the lateral (LPZ) and medial (MPZ) proliferation zones containing olfactory projection (Cluster 10) and local (Cluster 9) interneurons (Figure 1A) (Schmidt and Demuth, 1998; Beltz and Sandeman, 2003). In the brains of crayfish (*C. destructor, P. clarkii*) and clawed lobsters (*H. americanus*) the two proliferation zones are connected by long processes of cells whose nuclei reside in a niche located on the ventral surface of the accessory lobe, located roughly mid-way between the LPZ and MPZ (Figure 1B; Sullivan et al., 2007a); short processes of these niche cells project towards a vascular cavity that is the central feature in the niche (Figure 1C). The cytoplasm of the niche cells in *P. clarkii* is glutamine synthetase (GS)-positive (Figure 1B). The niche cells produce daughters that migrate along the GS-positive processes from the neurogenic niche towards the MPZ and LPZ, as revealed by double nucleoside labeling methods, forming migratory streams (Figure 1D; Sullivan et al., 2007a). Similar migratory streams have been observed in several other crustacean species, including *C. destructor*, *H. americanus* (Sullivan et al., 2007) and *Coenobita clypeatus* (Harzsch S and Hansson W, unpublished data). Once in close proximity to the proliferation zones in Clusters 9 and 10, these intermediate precursor cells divide at least once more before their descendants differentiate into neurons (Sullivan and Beltz, 2005).

The goal of this study was to advance our understanding of (1) the differential proliferative activity among the niche precursors with growth and aging, (2) the morphological characteristics of cells in the neurogenic niche and migratory streams, and (3) the cell cycle of migratory precursors. Our results show a progressive loss of proliferative capacity of the niche precursor cells in mature animals relative to young adults. A morphologically symmetrical division of neural precursor cells was observed near the point where the migratory streams emerge from the niche; symmetrically dividing cells also have been observed at the ends of the streams proximal and distal to the niche, and in the proliferation zones. A detailed examination of the migratory precursors revealed significant nuclear elongation and distortion during migration, consistent with nucleokinesis during directed movement. Nucleokinesis is a conserved pattern of neuronal precursor migration observed in many species both during development and in adulthood, and during tangential and radial migrations (Bellion et al., 2005; Tsai and Gleeson, 2005; Metin et al., 2007). During nucleokinesis, the nuclei of migrating neural precursor cells translocate in a saltatory fashion that is associated with nuclear elongation and distortion (Tsai et al., 2007), a process that involves cytoskeleton reorganization and motor protein coordination (Causeret et al., 2004; Higginbotham and Gleeson, 2007; Schaar and McConnell, 2005). The molecules Lissencephaly1 (LIS1) and doublecortin (DCX) appear to be important for migration through their interaction with the cytoplasmic dynein and microtubule complex (Friocourt et

Author Manuscript Author Manuscript Author Manuscript Author Manuscript

al., 2007; Morris et al., 1998; Tsai et al., 2007). In this paper we present evidence that the highly conserved protein LIS1 is expressed in cells in the migratory stream and neurogenic niche, implicating a role for this protein in the translocation of neural precursor cells in the crustacean brain. The symmetrical divisions of the niche precursors and migration of both daughters raises the questions of how the niche precursors are replenished as they divide and migrate away, and how their numbers increase with age. We explore here preliminary morphological evidence for an association between cells in the vasculature and the niche precursors in relation to these questions.

Materials and Methods

Animals and tissue processing

Freshwater crayfish *P. clarkii* (Malacostraca, Decapoda, Astacidae) of both sexes were obtained from Carolina Biological Supply Company (Burlington, NC) and maintained at 21°C in aquaria with recirculating artificial pond water and a light:dark cycle of 12:12 hours. For these studies, brains from three sizes of adult animals having carapace lengths (CL) of 5-6mm (Group 1), 9-14mm (Group 2) and 35mm (Group 3) were used. Group 1 animals were juveniles (ADII); Groups 2 and 3 were sexually mature.

For immunocytochemistry, brains were dissected in cold crayfish saline (205 mM NaCl, 5.4 mM KCl, 34.4 mM $CaCl_2$, 1.2 mM $MgCl_2$ and 2.4 mM $NaHCO_3$) and then fixed (4% w/v paraformaldehyde in 0.1 M phosphate buffer [PB, 20 mM NaH_2PO_4, 80 mM Na_2HPO_4 and pH 7.4]) at 4°C for 16 hours. In most cases, immunostaining was performed on whole mounted brain tissues. For immunohistochemistry on cryosections, tissue samples were immersed in 4% w/v paraformaldehyde overnight and then soaked in cryoprotectant (30% w/v sucrose in PB) at 4°C for 16 hours. The tissue blocks were embedded in Tissue Freezing Medium™ (Jung, Germany) and then cryo-sectioned (Leica cryostat Jung CM-3050, Germany) to a nominal thickness of 20 μm. Sections were mounted onto SuperFrost® Plus Micro Slides (VWR international, PA) and kept at –80°C until further processing.

For plastic sections, small pieces of brain tissue containing the migratory stream, the neurogenic niche and the vascular cavity were dissected from crayfish (20-25 mm CL). Tissues were fixed in a solution containing 4% paraformaldehyde, 2.5% glutaraldehyde and 0.5% tannic acid in cacodylate buffer pH 7.2. The material was then post-fixed in 1% osmium tetroxide, dehydrated in a graded ethanol series, and infiltrated and embedded in Spurr resin. Semi-thin sections (0.5 μm) were obtained with with a Sorvall MT-5000 ultramicrotome (DuPont de Nemours & Co., Wilmington, DE) and stained with a mixture of toluidine blue and borax.

BrdU labeling

To label proliferating cells, animals with carapace lengths of less than 20 mm were maintained in the S phase marker 2 mg/ml 5-bromo-2′-deoxyuridine (BrdU; Sigma, St. Louis, MO; No. B5002) in crayfish saline at 21°C for 8 hours. For animals bigger than 20 mm in carapace length, a single injection of BrdU (0.1ml of 5 mg/ml BrdU per cm CL) into

Author Manuscript Author Manuscript Author Manuscript Author Manuscript

the pericardium was made, and animals were then maintained in artificial pond water at 21°C for 8 hours prior to dissection and fixation.

Immunohistochemistry

Fixed whole mount brains or brain sagittal cryosections from BrdU-treated animals were rinsed multiple times with PB, incubated with 2N HCl for 45 min, and then rinsed with 0.3% Triton X-100 in PB (PBTx) for 1.5 hours. Samples were incubated for 16 hours at 4°C with primary antibodies mouse anti-GS (1:100; BD Biosciences Pharmingen, San Jose, CA; No. 610517) and rat anti-BrdU (1:50; Accurate Chemical, Westbury, NY; No. OBT0030G). After rinsing with PBTx for 2 hours, samples were incubated with secondary antibodies of donkey anti-mouse Cy5 (1:100; Jackson Immunoresearch, West Grove, PA; No. 715-175-151) and donkey anti-rat Cy2 (1:100; Jackson Immunoresearch; No. 712-225-153) at 4°C for 16 hours in the dark. The samples were washed with PBTx for 3 hours and counterstained with propidium iodide (25 μg/ml in PB; Sigma) for 15 min. The brains or sections were then rinsed with PB and mounted with Gel/mount™ (Biomeda Corp., Foster City, CA) for viewing and image capture with a Leica TCS SP confocal microscope. For labeling mitotic cells, instead of anti-GS, the brains were sequentially incubated with rabbit anti-phosphohistone H3 (Ser 10; 1:200-1:500; Upstate Biotechnology, Lake Placid, NY; No. 06-570) and donkey anti-rabbit Cy3 (1:100; Jackson Immunoresearch, No.711-165-152), followed by immunocytochemical processing for BrdU as described above. Goat anti-LIS1 antibody (1:25-50; sc-7577) was obtained from Santa Cruz Biotechnology, Inc. (Santa Cruz, CA, USA) and secondary antibody donkey anti-goat Cy2 (1:100; No. 705-225-147) from Jackson Immunoresearch.

The GS antibody served as a glial marker, as reported in previous studies in crustaceans (Linser et al., 1997; Allodi et al., 2006). Monoclonal mouse anti-Elav (1:10; DSHB; No. Elav-9F8A9), a neuronal RNA binding protein (Robinow et al., 1988), was used in this study only as a histological reagent (Sullivan et al., 2007a) to outline the vascular cavity. BrdU incorporation and immunocytochemical detection labeled cells in S phase (Dolbeare, 1996), while mitotic cells were distinguished with the M-phase marker phosphohistone H3 (Canela et al., 2003). The specificity of these antibodies was verified by Western blot as reported in our previous study (Sullivan et al., 2007a). LIS1 antibody indicated a band around 45 kDa in both mouse and *P. clarkii* brain preparations (Figure 8E). The LIS1 staining pattern in the migratory stream and niche was abolished after antibody preabsorption with the immunogen, provided by Santa Cruz Biotechnology, Inc.

Western Blot

Brain samples were lysed with RIPA lysis buffer (50 mM Tris pH7.5, 150 mM NaCl, 1% Triton X-100, 1% Nadeoxycholate, 0.1% SDS and Halt proteinase inhibitor [Pierce, USA; No. 78430]). Total protein concentration was determined by the bicinchoninic acid (BCA) protein assay method (Pierce. No. 23227). Protein samples (30 μg total protein in each sample) separated by 4-15% SDS-PAGE were electroblotted onto a Immuno-PSQ PVDF membrane (0.2 μm, Millipore). The membrane was blocked with 4% skimmed milk in TBST buffer (10 mM Tris pH 8.0, 150 mM NaCl, 0.1% Triton X-100) for 1 hour at room temperature. Incubation with LIS1 antibody (1:200) was typically done for 16 hours at 4°C

Author Manuscript Author Manuscript Author Manuscript Author Manuscript

on a rocking platform. HRP-coupled donkey anti-goat antibody (Jackson Immunoresearch, No. 705-035-147) was added and incubated at 24°C for 1 hour. After washing, signals were developed by reaction with an enhanced chemiluminescence kit (Amersham Bioscience, USA. RPN2109) and visualized according to the manufacturer's instructions.

Microscopy and image analysis

Fluorophore-labeled specimens were visualized with a Leica TCS SP laser scanning confocal microscope equipped with argon 488 nm, krypton 561 nm and helium-neon 633 nm lasers. Serial optical sections were taken at intervals of 1 μm and saved as both three-dimensional stacks and two-dimensional projections. To examine BrdU-labeled cells in the niche and stream, the orthogonal slicer function in the Leica software was applied on image stacks, to provide sagittal (yz-axis) and coronal (xz-axis) views of the niche and stream. Plastic sections were viewed and photographed with a Nikon Eclipse 80i microscope.

Image preparation, assembly, and analysis were performed in Photoshop 7 (Adobe Systems, Inc., San Jose, CA). Only the color balance and contrast of the images were adjusted.

Data analysis and statistics

The numbers of cells in the niche and BrdU-labeled cells in the stream were counted from optical 3D stacks of images. A single optical section was projected onto the monitor and the labeled cells traced onto a transparent sheet. This was repeated for each optical section and the cell profiles then counted from the sheets. Only cells double-labeled with propidium iodide and glutamine synthetase, and located around the vascular cavity, were considered as niche cells. Cells with BrdU-labeled nuclei and GS-labeled cytoplasm, were considered to be proliferating neuronal precursor cells; cells with these staining properties were never seen outside of the niche and stream. The thickness of the stream was averaged from three measurements at proximal, distal and middle points of the stream, taken from confocal images of whole mount brains that were mounted with the ventral side of the brain towards the coverslip. The size of each niche was calculated as an average of the long and short axes of the niche. To calculate nuclear eccentricity, the major (2a) and minor (2b) axes (Figure 6A) of each nucleus were measured with the Leica software, and eccentricity calculated using the formula in Figure 6A. All data are presented as mean ± SEM. Comparisons between different groups of animals were made with one-way ANOVA analysis followed by Tukey's multiple comparison tests, using Prism software (GraphPad Software, Inc., San Diego, CA).

Results

Organization of the niche and migratory streams

Immunocytochemistry of whole mount and sectioned brains of all three size groups of animals revealed anti-GS staining in the cytoplasm and processes of cells in the neurogenic niche and migratory streams (Figures 1B and 2). Propidium iodide stained cells were considered to be in the niche or streams if the labeled nuclei were confined within the outline of the GS-labeled structures; sagittal and coronal views of orthogonal sections of each primary stack of optical images through the niche and streams enabled us to eliminate

Author Manuscript Author Manuscript Author Manuscript Author Manuscript

any GS-negative or BrdU-positive cells which were in the vicinity of the niche and streams, but not within these structures (Figure 2).

Sagittal cryosections through the brains of the largest crayfish (36 mm CL), labeled for BrdU, GS and propidium iodide, revealed the three-dimensional structure of the stream to resemble a belt running along the ventral surface of the brain at the level of the accessory lobe (Figure 3). Cells with BrdU-positive nuclei and GS-positive cytoplasm (filled arrowheads, Figures 2D, F and arrows in Figure 3B) were observable in the stream, as were occasional cells with longitudinal nuclei that were not BrdU-labeled (open arrowheads, Figure 2F). Propidium iodide also labeled cells (red) surrounding the streams, but these did not label with the BrdU or GS antibodies (Figure 2B, D, F and Figure 3B-D).

Increase in size of the niche and streams during the transition from juvenile to mature crayfish

An increase in the size of the niche (compare Figures 2A, C and E) and the niche precursor cells (data not shown) was observed with increasing carapace length. Detailed measurements of the niche revealed that the mean value of its two axes was 121.8 ± 10.58 μm in our Group 1 animals, 151.7 ± 13.66 μm for the Group 2 animals and up to 210.8 ± 11.22 μm for the Group 3 animals (mean ± SEM, Figure 4A). BrdU-positive neuronal precursor cells were observable within the niche in all three sizes of animals. These cells were slightly bigger than other GS-positive niche cells and were found in various locations, sometimes at the two ends of niche close to the emergence of the stream (Figure 2A and 2C), or embedded within the highly packed non-mitotic niche cells (Figure 2C, E). A significant increase in the width of stream was found with increasing animal size, when whole-mount brains were optically sectioned in the dorsal-ventral plane (compare Figure 2B, D and F). The width of the stream changed from 9.07 ± 0.79 μm in Group 1 animals, to 14.37 ± 1.18 μm in the Group 2 animals and to 24.55 ± 2.88 μm in the Group 3 animals (mean ± SEM, Figure 4B). In most cases, the streams in Group 1 crayfish were thin strands that are narrower than the nuclei of the migrating cells. In this youngest group of animals we also observed fine GS-positive processes running parallel to but outside the primary stream, with BrdU-labeled nuclei migrating along them; these additional streams were never seen in larger animals, perhaps suggesting that the migratory stream is still being established in the juvenile animals. The entire length of the stream, measured from the LPZ to MPZ on one side of the brain, also increases with animal size (Figure 4C), from 662.7 ± 44.4 μm in Group 1 to 1584 ± 50.6 μm in Group 3. With very few exceptions, BrdU-positive cells were lined up single file in the streams. Cells with a nuclear morphology similar to BrdU-positive cells, but which did not label for BrdU, were occasionally found in the streams (open arrowheads, Figure 2F). The position of the niche relative to the accessory lobe (AL) varies among individual animals (Figure 4D). However, the morphology and the length of the streams, and the location of the niches on the two sides of the same brain, were generally symmetrical.

The proliferation rate of niche neuronal precursor cells relative to animal size

To compare the proliferation rates in the adult neurogenic niche in the three different size groups of crayfish, immunostaining for GS and BrdU was combined with propidium iodide

Author Manuscript Author Manuscript Author Manuscript Author Manuscript

to reveal the neurogenic niche and migratory streams. The relative proportion of neuronal precursor cells in the different sizes of animals was calculated by counting the number of BrdU-labeled cells in the niche (or streams) and dividing this by the total number of niche or stream cells labeled with propidium iodide.

We find that the total numbers of cells in the niche increased significantly with animal size (Figure 5A), from 61.7 ± 4.3 in Group 1, 126.4 ± 7.5 in Group 2 to 276.4 ± 15.6 cells in Group 3 (mean ± SEM, $P<0.0001$ in one-way ANOVA). This result correlates with the finding that the size of the niche increases as the animals grow (see Figures 2 and 4). However, the proportion of S-phase cells, revealed by BrdU labeling, decreases with increasing animal size (Figure 5B). In the largest animals, 0-1 labeled cells were observed in the niche following the 8-hour BrdU exposure; we know from prior studies that several days of exposure to BrdU is necessary to reliably label niche cells in the largest/oldest animals (Sullivan et al., 2007a). These data suggest that the cell cycle of the niche precursors slows as the animals grow and age, a finding that is consistent with studies of adult neurogenesis in mammalian systems (Altman and Das, 1965; Kuhn et al., 1996; Cameron and McKay, 1999). Penetration of BrdU in the larger crayfish brains is not likely to be a limitation contributing to these results, as BrdU is injected directly into the pericardium in the larger animals; there is a direct connection between the vasculature and the niche (Figure 1C; Sullivan et al., 2007a), and there is no blood-brain barrier to prevent BrdU from gaining access to the niche (Abbott, 1972). In contrast to the large animals, 3 or more cells were labeled on average in each niche in Group 1 animals. Overall, the proportion of labeled cells in the niches of the Groups was 6.76 ± 1.9% in Group 1, 1.01 ± 0.3% in Group 2 and 0.4 ± 0.2% cells in Group 3 (Figure 5C). Similar trends in proliferation rates were also found when the numbers of cells in the niche and stream were pooled (Figure 5D). These results are consistent with the idea that although crayfish undergo life-long neurogenesis, younger crayfish have a higher proportion of actively dividing neuronal precursor cells than older animals (Harzsch et al., 1999).

Nuclear eccentricity and nucleokinesis in the stream during cell migration

We have shown previously with double nucleoside analogue-labeling (Figure 1D) that neuronal precursor cells migrate from the niche to the lateral and medial proliferation zones along the GS-labeled stream (Sullivan et al., 2007a). To explore this migration further, in the current study we have compared the morphologies of cells selected from the middle of the stream (A), cells still in the stream but very close to the proliferation zone in Cluster 9 or Cluster 10 (B), and cells in the proliferation zones (C) (Figure 6B). A fourth selection (D) was composed of propidium iodide-labeled cells that were not labeled with BrdU, and which were located close to (but not in) the stream. Since the nucleus of each cell is either similar to a circle or oval in shape, we reduced their morphologies to a standard ellipse. The nuclear eccentricity of the four groups of cells was then calculated according to the standard geometrical definition for an ellipse (Figure 6A), where eccentricity falls between 0 and 1, with a circle having an eccentricity of 0. Values approaching 1 indicate an increasing elongation of the nucleus.

Author Manuscript Author Manuscript Author Manuscript Author Manuscript

Visual inspection suggests that BrdU-labeled nuclei in the stream (selection A, Figure 6B) are generally more elongate than the nuclei of cells outside the stream (selection D, Figure 6B) (see also Figure 2D, F). Indeed, the histogram of nuclear eccentricity (Figure 6C) reveals that cells in the stream have a significantly different nuclear morphology than cells in all of the other groups ($P<0.0001$; one-way ANOVA). We observe a decrease in eccentricity in BrdU-labeled nuclei from the middle of the stream towards the proliferation zones (0.90 ± 0.01 in group A, 0.72 ± 0.04 in group B and 0.59 ± 0.05 in group C; data presented as mean ± SEM).

Statistical analyses reveal that $84 \pm 3.3\%$ of BrdU-labeled cells in the stream have a distinctive ellipsoidal nuclear morphology with the long axis aligned between the niche and proliferation zones (small arrows in Figure 7B). However, in addition to these elliptical nuclei, two types of distorted nuclei were found in the migratory stream: one with a wide head towards the proliferation zone and narrow end towards the niche (short arrow in Figure 7A), the other one with a reversed orientation (double arrowheads in Figure 7C). These distorted nuclei suggest that nucleokinesis may be occurring during neuronal precursor cell migration. In the vertebrate brain nuclear migration is saltatory; generally there is a brief time when the nucleus jumps forward and a relatively long pause between jumps. Only when the nucleus undergoes such a saltatory mode of translocation can such nuclear distortion be seen (Tsai et al., 2007). Consistent with these reports, the morphology of nuclei that are wide in front (towards the direction of migration) and narrow in the rear in the migratory streams may be cells that just completed nuclear translocation, while nuclei that are narrow in front and broader in the rear are probably the cells just before the translocation.

Cells in the niche and stream are immunoreactive for LIS1

LIS1 is a protein that interacts with cytoskeletal elements, and is important in the migration of neural precursor cells in mammals (Tsai et al., 2007). In the crayfish brain, an antibody against the LIS1 protein labels the cytoplasm of cells in the stream and niche (Figure 8). Punctate staining was observed in the cytoplasm of the niche precursor cells (Figure 8B) and in their processes composing the stream (Figure 8D); LIS1 co-labels with GS in these areas. LIS1 labeling is particularly intense near the vascular cavity (Figure 8B, C). No labeling was seen after LIS1 antibody was pre-absorbed with LIS1 blocking peptide (Santa Cruz, sc-7577p). Western blot revealed an immunopositive band (37-50 kDa) in brain preparations from crayfish of the three different sizes (Lane 1-3; Figure 8E); this molecular weight is close to the size of the mammalian LIS1 protein (lane 4, mouse brain tissue, ∼45 kDa).

Neuronal precursors undergo symmetrical cell divisions in the niche and streams

To further explore the cell cycle in neuronal precursor cells, we examined the position and pattern of dividing cells in the neurogenic niche and streams in *P. clarkii*. Following an 8-hour incubation in BrdU, cells in the process of telophase or cytokinesis, or paired cells that had recently divided, were seen labeled with BrdU in the niche near where the migratory streams emerge (Figure 9A-C [images of Group 3 crayfish], G-L [Group 1]) and in the streams themselves near the proliferation zones (Figure 9D-F [Group 1]). In these crayfish, therefore, the S, G2 and M phases of the cell cycle collectively take ≤8 hours. Cells with

Author Manuscript Author Manuscript Author Manuscript Author Manuscript

condensed DNA were observable close to both the lateral and medial proliferation zones as well as occasional cells in the streams that were in metaphase, with condensed chromosomes aligned in the middle of the cell (arrow, Figure 9F). In this same image, several BrdU-positive cells with elongated nuclei were also seen in the stream, suggesting that these cells are migrating towards Cluster 9. At the distal end of the stream near Cluster 10, a late anaphase or telophase cell was observed (Figure 9E). Serial confocal optical sections taken close to the niche in one brain show a cell that had almost completed cytokinesis (Figure 9G-L). One section (Figure 9K) shows a small area of cytoplasm that is still shared between the two emerging, geometrically symmetrical daughter cells. The cytoplasm of the dividing cells is GS-positive, a characteristic feature of the cells residing in the niche, thus confirming the ancestry of these cells.

Three observations related to cell divisions in this system are: (1) Divisions are always morphologically symmetrical, regardless of whether these occur in the niche, streams or proliferation zones. (2) While BrdU-labeled cells can be found anywhere in the niche, cell divisions occur near the emergence of the streams or in the streams themselves, suggesting that both daughters of the niche cells migrate; indeed many paired cells can be visualized in the streams. Mitotic figures have never been observed in the central region of the niche near the vascular cavity, nor among the tightly clustered niche cells. (3) When cytokinesis occurs while a cell is migrating in the stream, the cleavage planes are always perpendicular to the track of the stream (Figure 9; Figure 10F,G). The tendency for the cleavage plane to orient relative to the stream is maintained between the MPZ and Cluster 9 (Figure 9D-E, G), but not in Cluster 10 (Figure 10A-C, G) where random cleavage planes were found.

How is the niche precursor cell pool replenished and expanded?

The niche increases in size and contains increasing numbers of precursor cells as the animal grows. Our data show that these precursor cells often migrate while in S-phase and that they generally divide just prior to or during migration. The divisions of the niche precursor cells that we have observed are always geometrically symmetrical, and there are many examples showing that both daughter cells are in the migratory stream. Some important questions emerge from these findings: *i. Why isn't the supply of precursor cells in the niche depleted over time, as they divide and migrate away? ii. Is this a self-renewing population of cells, as might be expected? iii. By what mechanism do the numbers of niche precursor cells expand as the animal grows?*

The crayfish niche, like the neurogenic niches in mammals, is closely associated with the vasculature. Not only do the crayfish niche and streams lie directly on a blood vessel, there is also a connection between the niche and the blood system via the vascular cavity. Injection of labeled dextran into the dorsal artery that supplies the brain with hemolymph, followed by immediate fixation, demonstrated that the dextran fills the vascular cavity (Figure 1C; Sullivan et al., 2007a). This cavity is therefore the most likely gateway into the niche.

To begin to explore this possibility, semi-thin (0.5 μm) plastic sections stained with toluidine blue were examined more closely to observe the histological characteristics of the niche. The majority of cells (Type I) composing the niche contain nuclei that are cuboidal (Figure

Author Manuscript Author Manuscript Author Manuscript Author Manuscript

11A,B) or elliptical (Figure 11D) depending upon the orientation of the section; the nuclei are 3-8μm in their shortest, and 10-15μm in their longest dimension. A standard characteristic of these nuclei is a darkly-staining boundary with heterochromatin and a center with euchromatin and one or more nucleoli. The cytoplasm surrounding the nucleus forms extensions that contact the rim of the vascular cavity. Often there are vacuoles in the cytoplasm of the niche cells where they border the vascular cavity (Figure 11B). The edge of the vascular cavity is decorated with finger-like cytoplasmic processes of the niche cells. A second, apparently distinct cell type contains a roughly spherical, densely stained nucleus, and a cytoplasm that is less darkly stained than cell type I. The cytoplasm is often densely packed with small spherical-oval granules. These cells (Type II, Figure 11A) are found less frequently in the niche, but when they are seen these are distinct against the homogeneity of the much more common cell Type I. A third distinctive cell type (Type III, Figure 11A) contains a darkly and homogeneously stained spherical nucleus and clear cytoplasmic vesicles, and has an amoeboid shape.

We also examined the regions contiguous with the niche and channels that appear to connect the vascular cavity with the blood vessel on which the niche lies. Here we find cells that are of the same size and appearance as the niche Type I cells. These were found in the blood vessel connected to the vascular cavity (Figure 11D), as well as in small vessels in the nearby accessory lobe (Figure 11C).

A complete and thorough histological and ultrastructural investigation of the niche and associated vasculature is beyond the scope of this paper. Nevertheless we propose, based upon the distinctive features shared by the niche precursors and the vascular cells, their close proximity, and the access to the niche by the blood system, that niche precursor cells may be derived from cells associated with the circulatory system that enter the niche via the vascular cavity.

Discussion

The precursor cells that produce adult-born neurons in the crustacean brain reside in a niche that has several features in common with vertebrate niches. These include having progenitors with glial properties that function as both precursor and support cells, directed migration, close association with the brain vasculature, and specialized basal laminae (Sullivan et al., 2007a). The daughters of the niche precursors migrate along streams that are defined by long processes of the niche cells and which terminate at proliferation zones where the migratory cells divide at least once more. These intermediate precursor cells therefore represent an amplification stage which, as in vertebrates, allows a rapid expansion of the precursor pool derived from individual niche cells.

In exploring the morphological changes in the neurogenic niche and streams in animals of different size categories, we find that the dimensions of these structures increase as the animals grow. As the carapace lengthens by roughly a factor of seven, the overall size of the niche nearly doubles, the length of the stream more than doubles, and the stream width nearly triples (Figure 4). In the youngest animals we examined, the width of the stream was often smaller than the nucleus of a migrating cell. We also observed strands with single

Author Manuscript Author Manuscript Author Manuscript Author Manuscript

migrating cells separate from the primary stream, a situation never seen in the larger/older animals, suggesting that the migratory pathway was in the early stages of being established. Consistent with the expansion in the size of the niche, the number of niche precursor cells increases by a factor of four over the range of animal sizes included in this study (Figure 5A). Conversely, however, the number of BrdU-labeled cells in the niche of older animals is only about one third of the number observed in the youngest animals, and as a result the proliferation rate in the niche decreases by a factor of ten (Figure 5B,C). All of these findings are in accord with the published literature in a variety of species, which suggests that as animals grow and age, the production of new neurons declines (Kempermann, 2006).

The decline in neurogenesis with age can be reversed, however, by changes in the organism's living habits and environment. For instance, increased locomotory activity in aging mice increases the numbers of new neurons that survive (Van Praag et al., 2005), a situation that also is true in crayfish (Sandeman DC, unpublished results). The fact that the proliferation rate following increased activity in mice or crayfish is stable, while the survival rate is altered, indicates that physical activity is influencing neurogenesis downstream from the precursor cell population. However, in other cases, life style changes can influence the rate of proliferation itself. For instance, a diet enriched in omega-3 fatty acids increases the basal levels of neurogenesis in the crustacean (lobster) brain (Beltz et al., 2007). In situations where the proliferation rate has been shown to increase due to environmental factors, it is not known whether this increase represents a change only in the cycling of the existing pool of precursors, or whether the precursor pool itself is expanded. The data provided by the present study can serve as a baseline for comparison, that will allow us to determine which cells in the precursor lineage are altered by environmental or endogenous factors. For instance, we can now determine whether diet alters the size of the precursor cell pool and/or their proliferation rate, or whether the change is downstream at the level of the numbers of divisions completed by the migratory “amplifying” precursors.

While the growth of crayfish is associated with increased size of the niche and streams, the position of the niche relative to the brain accessory lobes remains somewhat variable. In the youngest animals the niche is positioned in any quadrant on the ventral surface of the spherical ALs, while in the oldest animals the niches were confined to the medial half of the AL, and were most likely to be positioned centrally in the anterior-posterior plane. These data suggest that while the location of the niche stabilizes to some degree with age, this position is not fixed. In a review focused on the mammalian neurogenic niche the authors raise this issue, suggesting that niches may be “dynamic structures that alter their location and characteristics over time” (Riquelme et al., 2008). Our data corroborate this idea, and this feature is yet another point of comparison where the neurogenic niche in an invertebrate brain appears to share features that characterize the vertebrate niche. These many similarities suggest that adult neurogenesis is governed by common ancestral mechanisms that have been retained in a phylogenetically broad group of species.

Features of migrating precursors in the crustacean brain also resemble those of migratory precursors in vertebrate brains. The nuclei of migrating cells tend to be elongate (Figure 6) and undergo shape changes consistent with nucleokinesis (Figure 7), a cycle of nuclear elongation and distortion whereby nuclei translocate in a saltatory fashion. This mechanism

Author Manuscript Author Manuscript Author Manuscript Author Manuscript

is widely employed by migrating neuronal precursors in the vertebrate brain during development and in adulthood, and during both tangential and radial migrations. The shape changes we report suggest changes in cytoskeletal organization, and the presence of LIS1 immunoreactivity in the niche precursor cells and in their fibers composing the stream (Figure 8), supports this idea. LIS1 is a dynein-binding protein that is required for dynein activity. Not surprisingly, therefore, this molecule has been implicated in many processes involving the cell cycle and migration. For instance, LIS1 is involved in spindle assembly and centrosome separation (Tanenbaum et al., 2008), influences the timing of nuclear envelope breakdown in neural stem cells (Hebbar et al., 2008) and is involved in transport of cytoplasmic dynein during cell migration, a process that contributes to cytoskeletal coordination (Yamada et al., 2008). While the specific roles of LIS1 in our system are not yet understood, the distribution of this molecule and its concentration at the margins of the vascular cavity implicate potential roles in the behavior of the niche cells, their cell cycle and the migration of their daughters.

The niche cells divide in a morphologically symmetrical fashion to produce migratory daughters (Figures 9 and 10). While S-phase can occur in any position within the niche precursor cluster, GS-positive cells in M-phase have been observed only at the margins of the niche near the emergence of the streams or in the proximal parts of the stream (Figures 9A-C, G-L, 10F). Following this division, both daughters appear to migrate, and we see frequent examples of paired cells traveling in the parts of the stream proximal to the niche. There are also additional divisions of these migratory precursors near and in the proliferation zones; at least one but potentially two or more divisions are possible in these areas based on quantitative assessments of cell divisions over time (Benton and Beltz, 2001).

The symmetrical divisions of the precursors and migration of both daughters place us in a quandary: we know that with the growth of the animal, the number of niche precursors increases (Figure 5A). Why isn't the pool of niche precursors depleted over time, as these cells divide and migrate? Further, how is this pool augmented with growth? We have entertained three possible scenarios that could fill this gap in our knowledge. *Hypothesis #1:* The niche precursor cells can at certain times undergo unequal cell divisions to yield one migratory daughter and a larger cell that would remain in the niche (e.g. Schmidt, 2007), providing the self-renewing capacity that is lacking in our current model. We rule out this first option because we have no evidence that the niche precursor cells ever divide asymmetrically. Further, in order for asymmetric divisions to produce the requisite numbers of cells to maintain and expand the niche precursor pool, cell cycling would need to be continuous and therefore should have been very apparent in our studies. *Hypothesis #2:* There is a pool of cells in the niche that divide symmetrically, but the daughters remain in the niche instead of migrating away. Symmetrical division of stem-type cells is now acknowledged in some systems (Morrison and Kimble, 2006), so that "..the population itself is self-renewing and multipotent, but that no individual cell must necessarily hold these properties" (Magnus et al., 2008). Our immunocytochemical data suggest that the niche cells are a homogenous group of cells in terms of their shape and size, except when a cell is expanding during S and G2 phases, in preparation for mitosis. Further, the divisions of niche precursors that we have observed only occur in the niche near the origins of the streams or in

Author Manuscript Author Manuscript Author Manuscript Author Manuscript

the streams themselves, suggesting that the daughters of the niche cells are migratory; we also know that these migratory precursors will divide at least once more when they reach the proliferation zones, with a function similar to the transit amplifying cells of the mammalian brain. This second hypothesis therefore also seems unlikely. The basic problem with the first two scenarios, then, is that while we have observed many niche precursor cells in the process of cytokinesis, mitotic figures have only been seen near where the streams emerge from the niche, or in the streams themselves. We therefore have no evidence in favor of the niche precursor pool being a closed, self-renewing population.

The third option we have explored is that the niche is *not* a closed population, but rather that an external source could re-supply and expand the existing precursor pool (*Hypothesis #3*). One possibility is that cells from an unidentified source could migrate along the streams in the reverse direction ----*towards* the niche. We can discount this because we have done extensive double nucleoside labeling in order to determine the direction of migration of cells in the stream (Sullivan et al., 2007a, and Benton JL, unpublished results). In no case have we seen any evidence for cells migrating into the niche from the streams, or from the area surrounding the niche. We believe, therefore, that the only available access to the niche is via the vascular cavity. Although these data provide only a preliminary perspective on this issue, our semi-thin sections show that the niche cells have many cytological features in common with cells found in the nearby blood vessels. They are of a similar size, both vascular and Type I niche cells contain relatively large nuclei with multiple darkly-staining nucleoli, and the cytoplasm of both cell types often contains small refractile granules. The size and shape of “perivascular cells” and their similarity to cells in the niche of *Panulirus argus* have been previously noted (Schmidt, 2007).

Therefore, the cytological features of the niche cells are unusual, and yet these unusual characteristics are shared with cells in the vasculature. All three cell types in the niche resemble cells previously characterized in crustacean hematopoietic tissues and blood (George and Nichols, 1948; Abbott, 1971; Lanz et al., 1993; Chaga et al., 1995; Zhang et al., 2006); whether the vascular cells of interest in *P. clarkii* are hemocytes or perivascular cells remains to be determined. Based on these findings, we propose that the connection between the blood system and the crustacean neurogenic niche may be more than the supportive (e.g., nutrients) and instructive (e.g., hormones, cytokines and other circulating factors) roles that have been widely acknowledged in the vertebrates (Riquelme et al., 2008). Could cells associated with the circulatory system be transformed to become precursor cells in the neurogenic niche, that will ultimately generate the lineage of cells that produces neurons in the adult brain?

We have reported previously that the precursor cells in the neurogenic niche of the crayfish brain have glial properties (Sullivan et al., 2007a). These include their spindle-shaped structure, which features a large nucleus and two cytoplasmic processes. The shorter process extends towards and contacts the vascular cavity that is located centrally in the niche, terminating in a small endfoot; a long process projects towards the proliferation zone in either Cluster 9 or Cluster 10, forming the streams along which the daughters of the niche precursor cells migrate. The niche cells in the crayfish *P. clarkii* also label immunocytochemically with an antibody generated against glutamine synthetase, an enzyme

Author Manuscript Author Manuscript Author Manuscript Author Manuscript

that is involved in maintaining the glutamate-glutamine cycle in vertebrate astrocytes (Norenberg and Martinez-Hernandez, 1979; Patel et al., 1985) and which has been used as a glial marker in the brains of vertebrates (Linser, 1985; Hertz and Zielke, 2004; Ari and Kálmán, 2008) and crustaceans (Linser et al., 1997; Allodi et al., 2006; Sullivan et al., 2007a). The niche cells differ from other brain glia in the close proximity of their soma and the fasciculation of their processes into tracts (Sullivan and Beltz, 2007a). Little is known about the cell biology of brain glia in decapods, so it remains unclear in what other ways these cells might be distinctive.

The niche cells in the crustacean brain are both neuronal precursor and support cells, as these are the cells whose daughters migrate along the streams formed by the processes of the niche precursors. In this regard, they appear to function in much the same capacity as the astrocytic precursors in the vertebrate brain (Merkle et al., 2004; Ihrie and Alvarez-Buylla, 2008). And, while their cytoarchitecture is highly reminiscent of cells found in the nearby vasculature, they also have properties consistent with a glial character. These two identities may not be incompatible. A growing body of evidence demonstrates that cells derived from one adult tissue can change their phenotype, suggesting that mature cells can be reprogrammed (“transdifferentiated”) for a new function (Sanchez-Ramos, 2002). Data from in vitro and transplantation studies support this idea, overturning the dogma that a cell committed to a specific fate cannot change its destiny. Most relevant to this discussion, mammalian bone marrow cells have a proclivity to migrate to the brain when infused into a host animal (Eglitis and Mezey, 1997; Kopen et al., 1999; Brazelton et al., 2000). Another technique involves grafting bone marrow cells into the brain, and in one study where these were grafted into the lateral ventricle they migrated throughout the brain, including areas undergoing active postnatal neurogenesis. The descendants of these cells express a variety of glial and neuronal markers, including GFAP and F4/80 (a microglial marker; Eglitis and Mezey, 1997), NeuN and NSE (Mezey et al., 2000), NeuN and GFAP (Mahmood et al., 2001), and MAP-2, NeuN and GFAP (Chen et al., 2001), and in some studies developed the characteristics of astrocytes (Kopen et al, 1999). In vitro, bone marrow cells have been induced by various means to form neurons (Sanchez-Ramos et al., 1998, 2000, 2001; Kohyama et al., 2001), and in one study the bone marrow-derived neurons responded to depolarizing stimuli, showing a rapid and reversible calcium increase in response to acetylcholine, a response characteristic of neurons (Kohyama et al., 2001). The identities of specific types of bone marrow cells that are the source of neurons and glia in these studies is not clear, because the cells in various experiments were prepared by different means, and some attempted to exclude hematopoietic stem cells, while others did not. Other studies specifically used hematopoietic cells, and found that in the brain these could acquire neural features and express neural genes (Goolsby et al., 2003; Gottschling et al., 2007). The mounting literature regarding mammalian systems is therefore clear in its basic message: cells derived from bone marrow can transdifferentiate into neurons and glia in response to signals in the brain environment, or in vitro. Furthermore, perivascular cells in humans (primarily pericytes) have now been identified as the source of mesenchymal stem cells in several organs including skeletal muscle, pancreas and placenta (Crisan et al., 2008).

Author Manuscript Author Manuscript Author Manuscript Author Manuscript

Studies in *Drosophila melanogaster* also suggest that glial cells and hemocytes are functionally and molecularly related. The gene *glial cells deficient/glial cells missing* (*glide/gcm*) directs the cell fate switch between neurons and glial cells by activating the glial developmental program in multipotent precursor cells of the nervous system. Bernardoni et al. (1997) show that *glide/gcm* is also expressed early and transiently during the differentiation of hemocytes. As in glial cells, *glide/gcm* plays an instructive role in hemocyte differentiation.

The suggestion, then, that hemocytes or perivascular cells in the crustacean brain might enter the vascular cavity and differentiate into neuronal precursor cells in the niche, is in line with a growing literature that suggests an intimate, perhaps transforming, relationship between cells associated with the blood and neurons. The crustacean neurogenic niche may be an ideal system in which the role of vascular cells in adult neurogenesis can be tested in vivo. The niche is accessible, the lineage of cells leading to the production of new neurons has been defined, and the entire assembly line producing adult neurons can be dissected intact from the ventral surface of the brain, or observed in a single thick slice from the ventral surface of the brain. Our next studies in the crustacean brain will explore the ultrastructural characteristics of the niche precursors and the vascular cells, and will test whether cells labeled in hematopoietic tissues can be incorporated into the niche, and ultimately whether this label can be detected in differentiated neurons in the brain.

Acknowledgments

We thank P. Carey and V. LePage for care of the animals used in these studies, J.L. Benton for technical support, and C. R. Kirkhart for the image in Figure 10F. This work was funded by NIH R01 MH67157, NSF-IBN 0344448 and NSF-IOS 0818259 to B.S. Beltz, and a fellowship from CAPES/Ministry of Education of Brazil to S. Allodi (BEX 1177/08-7), to support her work while on leave in the Beltz Lab.

References

Abbott NJ. The organization of the cerebral ganglion in the shore crab, *Carcinus maenas*. II. The relation of intracerebral blood vessels to other brain elements. Z Zellforsch Mikrosk Anat. 1971; 120:401–420. [PubMed: 5151348]

Abbott NJ. Access of ferritin to the interstitial space of *Carcinus* brain from the intracerebral blood vessels. Tissue Cell. 1972; 4:99–104. [PubMed: 4647366]

Allodi S, Bressan CM, Carvalho SL, Cavalcante LA. Regionally specific distribution of the binding of anti-glutamine synthetase and anti-S100 antibodies and of *Datura stramonium* lectin in glial domains of the optic lobe of the giant prawn. Glia. 2006; 53:612–620. [PubMed: 16435368]

Altman J, Das GD. Autoradiographic and histologic evidence of postnatal neurogenesis in rats. J Comp Neurol. 1965; 124:319–335. [PubMed: 5861717]

Ari C, Kálmán M. Evolutionary changes of astroglia in Elasmobranchii comparing to amniotes: a study based on three immunohistochemical markers (GFAP, S-100, and glutamine synthetase). Brain Behav Evol. 2008; 71:305–324. [PubMed: 18446022]

Bellion A, Baudoin JP, Alvarez C, Bornens M, Metin C. Nucleokinesis in tangentially migrating neurons comprises two alternating phases: forward migration of the Golgi/centrosome associated with centrosome splitting and myosin contraction at the rear. J Neurosci. 2005; 25:5691–5699. [PubMed: 15958735]

Beltz BS, Sandeman DC. Regulation of life-long neurogenesis in the decapod crustacean brain. Arthropod Struct Dev. 2003; 32:39–60. [PubMed: 18088995]

Beltz BS, Tlusty MF, Benton JL, Sandeman DC. Omega-3 fatty acids upregulate adult neurogenesis. Neurosci Lett. 2007; 415:154–158. [PubMed: 17240063]

Author Manuscript Author Manuscript Author Manuscript Author Manuscript

Benton J, Beltz B. Effects of serotonin depletion on local interneurons in the developing olfactory pathway of lobsters. J Neurobiol. 2001; 46:193–205. [PubMed: 11169505]

Benton JL, Goergen EM, Rogan SC, Beltz BS. Hormonal and synaptic influences of serotonin on adult neurogenesis. Gen Comp Endocrinol. 2008; 158:183–190. [PubMed: 18692503]

Brazelton TR, Rossi FM, Keshet GI, Blau HM. From marrow to brain: expression of neuronal phenotypes in adult mice. Science. 2000; 290:1775–1779. [PubMed: 11099418]

Cameron HA, McKay RD. Restoring production of hippocampal neurons in old age. Nat Neurosci. 1999; 2:894–897. [PubMed: 10491610]

Canela N, Rodriguez-Vilarrupla A, Estanyol JM, Diaz C, Pujol MJ, Agell N, Bachs O. The SET protein regulates G2/M transition by modulating cyclin B-cyclin-dependent kinase 1 activity. J Biol Chem. 2003; 278:1158–1164. [PubMed: 12407107]

Causeret F, Hidalgo-Sanchez M, Fort P, Backer S, Popoff MR, Gauthier-Rouviere C, Bloch-Gallego E. Distinct roles of Rac1/Cdc42 and Rho/Rock for axon outgrowth and nucleokinesis of precerebellar neurons toward netrin 1. Development. 2004; 131:2841–2852. [PubMed: 15151987]

Chaga O, Lignell M, Söderhäll K. The haemopoietic cells of the freshwater crayfish, *Pacifasticus leniusculus*. Anim Biol. 1995; 4:59–70.

Chen CJ, Liao SL, Chen WY, Hong JS, Kuo JS. Cerebral ischemia/reperfusion injury in rat brain: effects of naloxone. Neuroreport. 2001; 12:1245–1249. [PubMed: 11338200]

Crisan M, Yap S, Casteilla L, Chen CW, Corselli M, Park TS, Andriolo G, Sun B, Zheng B, Zhang L, Norotte C, Teng PN, Traas J, Schugar R, Deasy BM, Badylak S, Bühring HJ, Giacobino JP, Lazzari L, Huard J, Péault B. A perivascular origin for mesenchymal stem cells in multiple human organs. Cell Stem Cell. 2008; 3:301–313. [PubMed: 18786417]

Dolbeare F. Bromodeoxyuridine: a diagnostic tool in biology and medicine, Part III. Proliferation in normal, injured and diseased tissue, growth factors, differentiation, DNA replication sites and in situ hybridization. Histochem J. 1996; 28:531–575. [PubMed: 8894660]

Eglitis MA, Mezey E. Hematopoietic cells differentiate into both microglia and macroglia in the brains of adult mice. Proc Natl Acad Sci U S A. 1997; 94:4080–4085. [PubMed: 9108108]

Friocourt G, Liu JS, Antypa M, Rakic S, Walsh CA, Parnavelas JG. Both doublecortin and doublecortin-like kinase play a role in cortical interneuron migration. J Neurosci. 2007; 27:3875–3883. [PubMed: 17409252]

George WC, Nichols J. A study of the blood of some Crustacea. J Morphol. 1948; 83:425–443. [PubMed: 18098431]

Gheusi G, Lledo PM. Control of early events in olfactory processing by adult neurogenesis. Chem Senses. 2007; 32:397–409. [PubMed: 17404148]

Goolsby J, Marty MC, Heletz D, Chiappelli J, Tashko G, Yarnell D, Fishman PS, Dhib-Jalbut S, Bever CT Jr, Pessac B, Trisler D. Hematopoietic progenitors express neural genes. Proc Natl Acad Sci U S A. 2003; 100:14926–14931. [PubMed: 14634211]

Gottschling S, Eckstein V, Saffrich R, Jonas A, Uhrig M, Krause U, Seckinger A, Miesala K, Horsch K, Straub BK, Ho AD. Primitive and committed human hematopoietic progenitor cells interact with primary murine neural cells and are induced to undergo self-renewing cell divisions. Exp Hematol. 2007; 35:1858–1871. [PubMed: 17697743]

Harzsch S, Miller J, Benton J, Beltz B. From embryo to adult: persistent neurogenesis and apoptotic cell death shape the lobster deutocerebrum. J Neurosci. 1999; 19:3472–3485. [PubMed: 10212307]

Hebbar S, Mesngon MT, Guillotte AM, Desai B, Ayala R, Smith DS. Lis1 and Ndel1 influence the timing of nuclear envelope breakdown in neural stem cells. J Cell Biol. 2008; 182:1063–1071. [PubMed: 18809722]

Hertz L, Zielke HR. Astrocytic control of glutamatergic activity: astrocytes as stars of the show. Trends Neurosci. 2004; 27:735–743. [PubMed: 15541514]

Higginbotham HR, Gleeson JG. The centrosome in neuronal development. Trends Neurosci. 2007; 30:276–283. [PubMed: 17420058]

Ihrie RA, Alvarez-Buylla A. Cells in the astroglial lineage are neural stem cells. Cell Tissue Res. 2008; 331:179–191. [PubMed: 17786483]

Author Manuscript Author Manuscript Author Manuscript Author Manuscript

Kaslin J, Ganz J, Brand M. Proliferation, neurogenesis and regeneration in the non-mammalian vertebrate brain. Philos Trans R Soc Lond B Biol Sci. 2008; 363:101–122. [PubMed: 17282988]

Kempermann, G. Adult Neurogenesis: Stem Cells and Neuronal Development in the Adult Brain. Oxford University Press; 2006.

Kohyama J, Abe H, Shimazaki T, Koizumi A, Nakashima K, Gojo S, Taga T, Okano H, Hata J, Umezawa A. Brain from bone: efficient "meta-differentiation" of marrow stroma-derived mature osteoblasts to neurons with Noggin or a demethylating agent. Differentiation. 2001; 68:235–244. [PubMed: 11776476]

Kopen GC, Prockop DJ, Phinney DG. Marrow stromal cells migrate throughout forebrain and cerebellum, and they differentiate into astrocytes after injection into neonatal mouse brains. Proc Natl Acad Sci U S A. 1999; 96:10711–10716. [PubMed: 10485891]

Kuhn HG, Dickinson-Anson H, Gage FH. Neurogenesis in the dentate gyrus of the adult rat: age-related decrease of neuronal progenitor proliferation. J Neurosci. 1996; 16:2027–2033. [PubMed: 8604047]

Lanz H, Tsutsumi V, Arechiga H. Morphological and biochemical characterization of *Procambarus clarkii* blood cells. Dev Comp Immunol. 1993; 17:389–397. [PubMed: 8270091]

Linser PJ. Multiple marker analysis in the avian optic tectum reveals three classes of neuroglia and carbonic anhydrase-containing neurons. J Neurosci. 1985; 5:2388–2396. [PubMed: 2863336]

Linser PJ, Trapido-Rosenthal HG, Orona E. Glutamine synthetase is a glial-specific marker in the olfactory regions of the lobster (Panulirus argus) nervous system. Glia. 1997; 20:275–283. [PubMed: 9262232]

Magnus T, Liu Y, Parker GC, Rao MS. Stem cell myths. Philos Trans R Soc Lond B Biol Sci. 2008; 363:9–22. [PubMed: 17284414]

Mahmood A, Lu D, Yi L, Chen JL, Chopp M. Intracranial bone marrow transplantation after traumatic brain injury improving functional outcome in adult rats. J Neurosurg. 2001; 94:589–595. [PubMed: 11302657]

Merkle FT, Tramontin AD, Garcia-Verdugo JM, Alvarez-Buylla A. Radial glia give rise to adult neural stem cells in the subventricular zone. Proc Natl Acad Sci U S A. 2004; 101:17528–17532. [PubMed: 15574494]

Metin C, Alvarez C, Moudoux D, Vitalis T, Pieau C, Molnar Z. Conserved pattern of tangential neuronal migration during forebrain development. Development. 2007; 134:2815–2827. [PubMed: 17611228]

Mezey E, Chandross KJ, Harta G, Maki RA, McKercher SR. Turning blood into brain: cells bearing neuronal antigens generated in vivo from bone marrow. Science. 2000; 290:1779–1782. [PubMed: 11099419]

Morris SM, Albrecht U, Reiner O, Eichele G, Yu-Lee LY. The lissencephaly gene product Lis1, a protein involved in neuronal migration, interacts with a nuclear movement protein, NudC. Curr Biol. 1998; 8:603–606. [PubMed: 9601647]

Morrison SJ, Kimble J. Asymmetric and symmetric stem-cell divisions in development and cancer. Nature. 2006; 441:1068–1074. [PubMed: 16810241]

Norenberg MD, Martinez-Hernandez A. Fine structural localization of glutamine synthetase in astrocytes of rat brain. Brain Res. 1979; 161:303–310. [PubMed: 31966]

Patel AJ, Weir MD, Hunt A, Tahourdin CS, Thomas DG. Distribution of glutamine synthetase and glial fibrillary acidic protein and correlation of glutamine synthetase with glutamate decarboxylase in different regions of the rat central nervous system. Brain Res. 1985; 331:1–9. [PubMed: 2859090]

Riquelme PA, Drapeau E, Doetsch F. Brain micro-ecologies: neural stem cell niches in the adult mammalian brain. Philos Trans R Soc Lond B Biol Sci. 2008; 363:123–137. [PubMed: 17322003]

Robinow S, Campos AR, Yao KM, White K. The elav gene product of Drosophila, required in neurons, has three RNP consensus motifs. Science. 1988; 242:1570–1572. [PubMed: 3144044]

Sanchez-Ramos J. The straight dope on addiction to dopamimetic drugs. Mov Disord. 2002; 17:223–225. [PubMed: 11835473]

Sanchez-Ramos J, Facca A, Basit A, Song S. Toxicity of dieldrin for dopaminergic neurons in mesencephalic cultures. Exp Neurol. 1998; 150:263–271. [PubMed: 9527896]

Author Manuscript Author Manuscript Author Manuscript Author Manuscript

Sanchez-Ramos J, Song S, Cardozo-Pelaez F, Hazzi C, Stedeford T, Willing A, Freeman TB, Saporta S, Janssen W, Patel N, Cooper DR, Sanberg PR. Adult bone marrow stromal cells differentiate into neural cells in vitro. Exp Neurol. 2000; 164:247–256. [PubMed: 10915564]

Sanchez-Ramos JR, Song S, Kamath SG, Zigova T, Willing A, Cardozo-Pelaez F, Stedeford T, Chopp M, Sanberg PR. Expression of neural markers in human umbilical cord blood. Exp Neurol. 2001; 171:109–115. [PubMed: 11520125]

Schaar BT, McConnell SK. Cytoskeletal coordination during neuronal migration. Proc Natl Acad Sci U S A. 2005; 102:13652–13657. [PubMed: 16174753]

Schmidt M. Continuous neurogenesis in the olfactory brain of adult shore crabs, Carcinus maenas. Brain Res. 1997; 762:131–143. [PubMed: 9262167]

Schmidt M. Identification of putative neuroblasts at the base of adult neurogenesis in the olfactory midbrain of the spiny lobster *Panulirus argus*. J Comp Neurol. 2007; 503:64–84. [PubMed: 17480012]

Schmidt M, Demuth S. Neurogenesis in the central olfactory pathway of adult decapod crustaceans. NY Acad Sci. 1998; 855:277–80.

Sullivan JM, Beltz BS. Newborn cells in the adult crayfish brain differentiate into distinct neuronal types. J Neurobiol. 2005; 65:157–170. [PubMed: 16114027]

Sullivan JM, Benton JL, Sandeman DC, Beltz BS. Adult neurogenesis: a common strategy across diverse species. J Comp Neurol. 2007a; 500:574–584. [PubMed: 17120293]

Sullivan JM, Sandeman DC, Benton JL, Beltz BS. Adult neurogenesis and cell cycle regulation in the crustacean olfactory pathway: from glial precursors to differentiated neurons. J Mol Histol. 2007b; 38:527–542. [PubMed: 17624620]

Tanenbaum ME, Macurek L, Galjart N, Medema RH. Dynein, Lis1 and CLIP-170 counteract Eg5-dependent centrosome separation during bipolar spindle assembly. Embo J. 2008; 27:3235–3245. [PubMed: 19020519]

Tsai JW, Bremner KH, Vallee RB. Dual subcellular roles for LIS1 and dynein in radial neuronal migration in live brain tissue. Nat Neurosci. 2007; 10:970–979. [PubMed: 17618279]

Tsai LH, Gleeson JG. Nucleokinesis in neuronal migration. Neuron. 2005; 46:383–388. [PubMed: 15882636]

Van Praag H, Shubert T, Zhao C, Gage FH. Exercise enhances learning and hippocampal neurogenesis in aged mice. J Neurosci. 2005; 25:8680–8685. [PubMed: 16177036]

Yamada M, Toba S, Yoshida Y, Haratani K, Mori D, Yano Y, Mimori-Kiyosue Y, Nakamura T, Itoh K, Fushiki S, Setou M, Wynshaw-Boris A, Torisawa T, Toyoshima YY, Hirotsune S. LIS1 and NDEL1 coordinate the plus-end-directed transport of cytoplasmic dynein. Embo J. 2008; 27:2471–2483. [PubMed: 18784752]

Zhang ZF, Shao M, Ho Kang K. Classification of haematopoietic cells and haemocytes in Chinese prawn *Fenneropenaeus chinensis*. Fish Shellfish Immunol. 2006; 21:159–169. [PubMed: 16480894]

Author Manuscript Author Manuscript Author Manuscript Author Manuscript

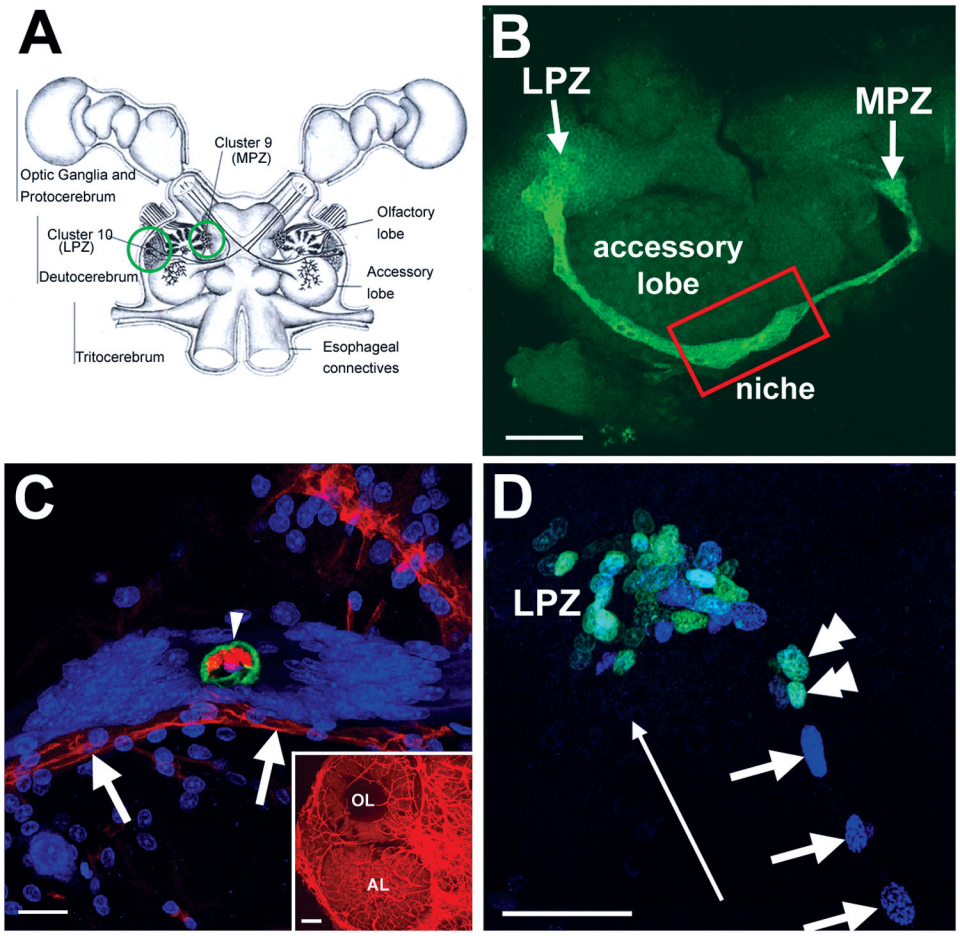

Figure 1.

Neurogenesis in the adult crayfish (*P. clarkii*) brain. A: Schematic diagram of the crayfish brain. Cell Clusters 9 and 10 (circled) flank the olfactory (OL) and accessory (AL) lobes of the deutocerebrum. B: The lateral proliferation zone (LPZ) in Cluster 10 and the medial proliferation zone (MPZ) in Cluster 9 are connected with each other on the ventral surface of the brain by a glutamine synthetase (green) labeled neurogenic niche and migratory streams. C: Dextran (red) injections into the dorsal artery show that the central region of the niche cell cluster, outlined by anti-Elav (green) labeling, is confluent with the vasculature (arrowhead); we have named this region the vascular cavity. Dextran labeling also shows that the niche and streams lie on a blood vessel (arrows). Propidium iodide (blue) labeling of the nuclei of niche cells is also shown. The inset shows dextran labeling of the vasculature of the olfactory (OL) and accessory (AL) lobes. D: Adult neuronal precursor cells migrate from the neurogenic niche along migratory streams towards two proliferation zones (PZ). The lateral proliferation zone (LPZ) shown here was revealed by BrdU (cyan; double arrowheads) and IdU (blue; arrows) sequential labeling, and demonstrates that the migrating cells are moving away from the niche and towards the proliferation zone (long arrow). Scale bars: 75 μm in B; 25 μm in C; 100 μm in inset of C; 40 μm in D (figure adapted from Sullivan et al., 2007a).

Author Manuscript Author Manuscript Author Manuscript Author Manuscript

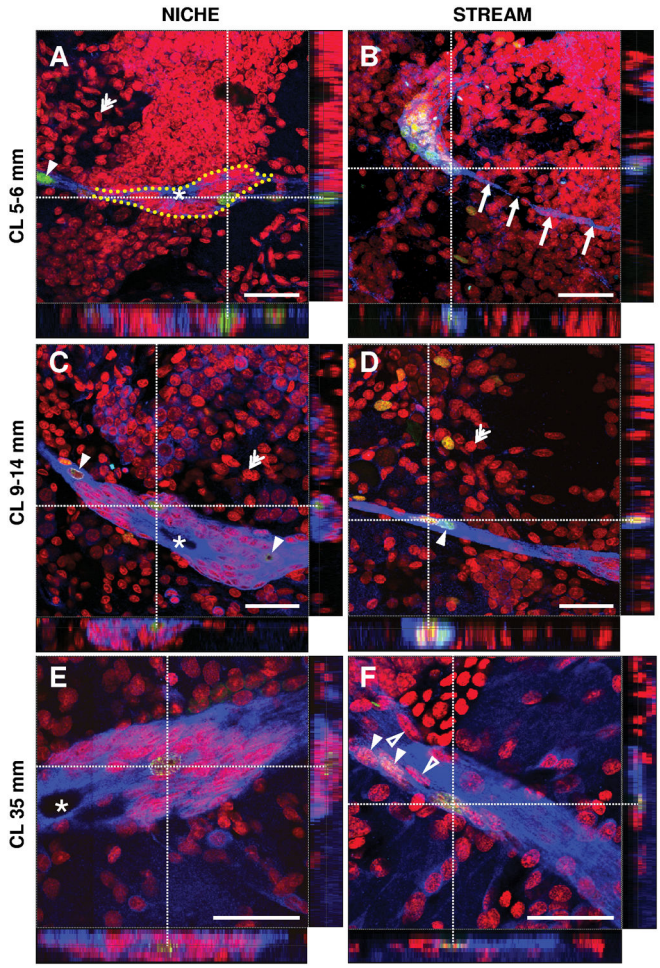

Figure 2.

Confocal images of the niches and streams of whole mount brains from three different size categories of adult *P. clarkii*. A-B: animals from Group 1, with an average carapace length (CL) of 5-6 mm; C-D: crayfish from Group 2 (9-14 mm CL) E-F: crayfish from Group 3 (35 mm CL). Animals were exposed to BrdU for 8 hours immediately before fixation. Double immunostaining shows BrdU (green) and glutamine synthetase (blue). Specimens were counterstained with the nuclear stain propidium iodide (red). The orthogonal slicer function of the Leica software was applied to each stack of images to obtain sagittal and coronal views of each image at the level of the white dotted reference lines. The intersection of the reference lines marks BrdU-labeled cells in the niches or the streams that were of particular interest and which can be seen in the Z axis at the bottom (xz-axis) and right side (yz-axis) of each figure. Filled arrowheads: BrdU- and GS-labeled glial cells in the stream and niche. The location of the niche is outlined in A by large yellow dots. Arrows in B point to the very narrow migratory stream (also labeled in blue). Double arrowheads: propidium iodide-stained cells outside of the stream and niche. Open arrowheads in F: Some elongated nuclei in the migratory stream were not labeled for BrdU. Asterisks in A, C and E: the vascular cavity. Scale bars =50 μm in all figures.

Author Manuscript Author Manuscript Author Manuscript Author Manuscript

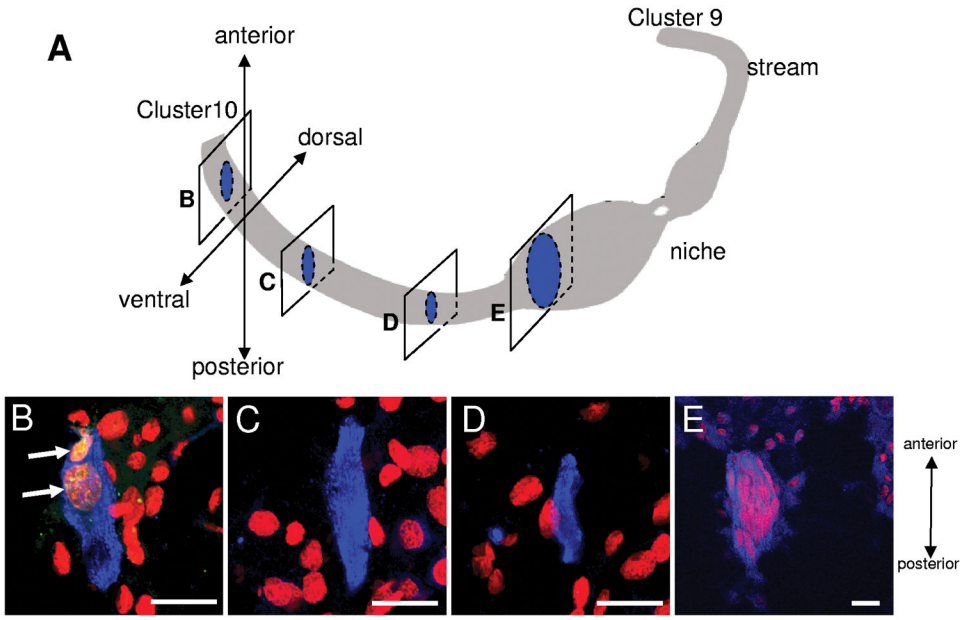

Figure 3.

Sagittal cryosections through the niche and stream of a 36mm CL (Group 3) crayfish brain revealed that the migratory streams form a belt-like structure on the ventral surface of the brain. Twenty-micron thick sections were double-labeled for BrdU (green) and glutamine synthetase (blue) and further counterstained with propidium iodide (red). A is a schematic diagram showing the positions of sagittal sections in B-E. The left side of each image (B-E) is towards the ventral side, and the top towards the anterior side of the brain. BrdU-labeled cells are seen still in the stream, in the section closest to the Cluster 10 proliferation zone (B) (arrows). Many BrdU-negative cells, labeled with propidium iodide (red) are found ventral and dorsal to the stream (B-D) and in the niche (E). Scale bars are 20 μm in all images.

Author Manuscript Author Manuscript Author Manuscript Author Manuscript

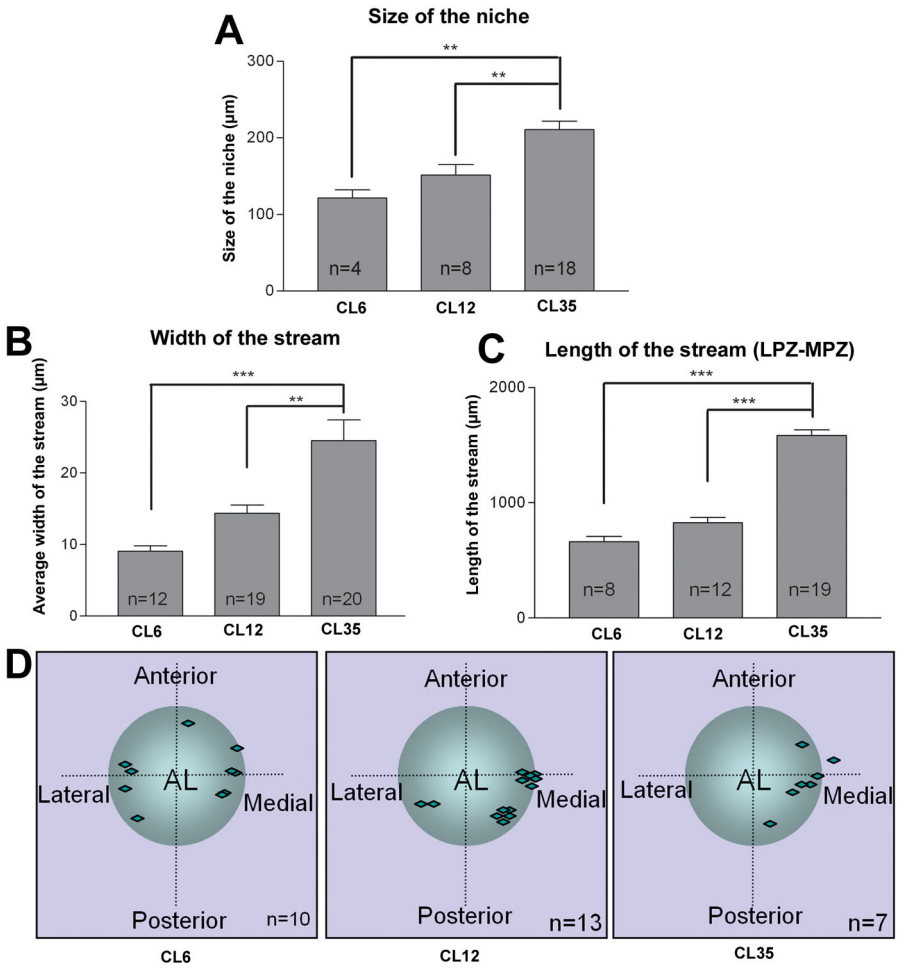

Figure 4.

Histogram showing the difference in size of the niches and streams with increasing animal size. Comparisons of the size of the niche (A), average width of the streams (B) and length of the streams from the LPZ to the MPZ (C) in the three different sizes of crayfish (CL, carapace length in mms indicated on the x-axes). D: Schematic diagram of the location of the niche relative to the accessory lobe (AL). The position of each vascular cavity is indicated with a diamond. The width of the stream, length of stream and size of niche increased significantly with the animal growth in size. ($P<0.0006$ for A, $P<0.0001$ for B and C by one-way ANOVA). Significant differences between groups are marked with double ($P<0.01$, Tukey comparison) and triple ($P<0.001$, Tukey comparison) asterisks. n = numbers of niches in A; numbers of streams in B and C; numbers of brain hemispheres in D.

Author Manuscript Author Manuscript Author Manuscript Author Manuscript

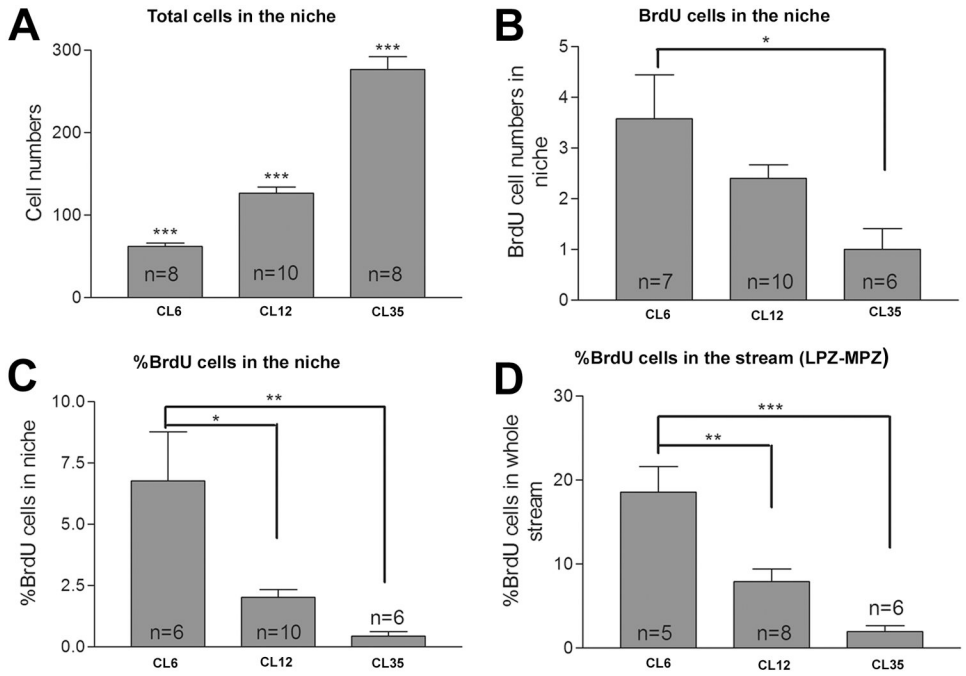

Figure 5.

Comparison of precursor cell total numbers, BrdU-labeled cells, and their relative proportions in the niches and the streams in different sizes of crayfish. The x-axis indicates the average carapace length (CL) in mm of the animals. Animals were exposed to BrdU for 8 hours prior to fixation, then immunolabeled for BrdU and glutamine synthetase and counterstained with propidium iodide. Total cell numbers and BrdU-labeled cells in the niches and streams were counted. Histograms A and B show the total numbers of cells and BrdU-positive cells in the niche respectively. The percentage of BrdU-labeled cells in the niche (C) or in the niche and stream combined (D) were normalized to the total number of propidium iodide-labeled cells in these structures. Note a significant decrease in the numbers (B) and percentages (C and D) of BrdU-labeled cells with increasing size ($P<0.004$ in C and $P<0.0001$ in D by one-way ANOVA). Significant difference between groups (Tukey multiple comparison) are marked with single ($P<0.05$), double ($P< 0.01$) or triple ($P<0.001$) asterisks. n = numbers of niches assayed in A-C; numbers of streams assayed in D.

Author Manuscript Author Manuscript Author Manuscript Author Manuscript

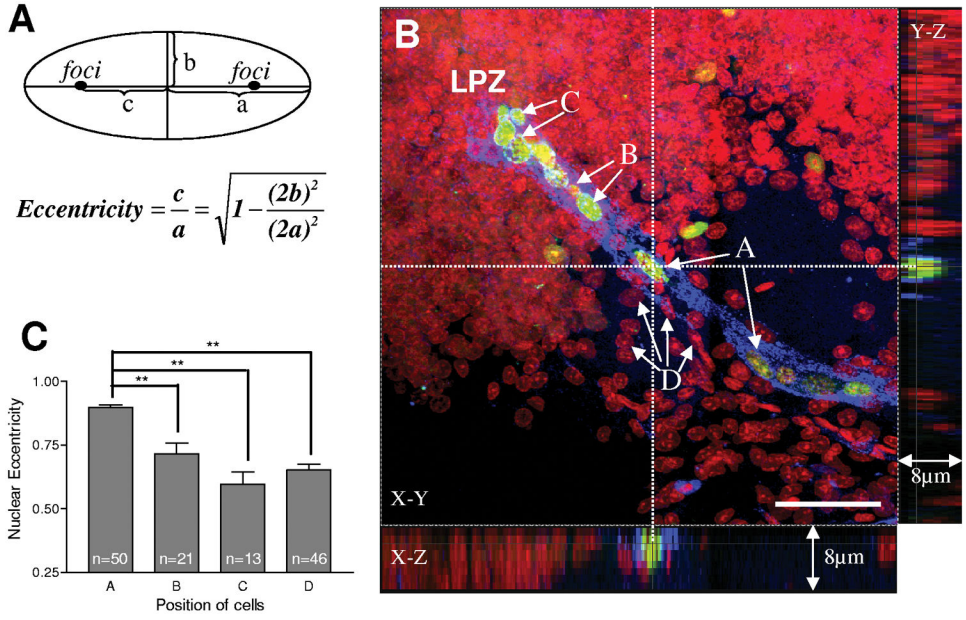

Figure 6.

Cells in the stream maintain a distinctive ellipsoidal nuclear morphology. The image in B is labeled for BrdU (green), glutamine synthetase (blue) and propidium iodide (red). A: the definition of nuclear eccentricity. a, semi-major axis of nuclei; b, semi-minor axis of nuclei; c, the distance from the center to the focus of the ellipse. B-C: BrdU positive cells are separated into three groups based on the location from which they were selected. A: cells from middle of the stream; B: cells located in the distal part of the stream close to proliferation zone; C: cells located within the proliferation zone. The elongation of BrdU-labeled cells was also compared with BrdU-unlabeled cells that were near to, but outside the stream (D). The orthogonal slicer function of the Leica software was applied in B to obtain sagittal and coronal views. The dotted reference lines indicate the plane of section for these views. The intersection of the reference line marks an elongated cell in the middle of the stream which is both BrdU and GS labeled and which can be seen in the Z axis at the bottom and right sides of the figure. Cells in the stream (A) show a statistically significant increase in nuclear elongation relative to the other groups. Scale bar =50 μm in B. Data analyzed with one-way ANOVA. $P<0.0001$ in C. Significant differences between groups (Tukey multiple comparison) are marked with double asterisks ($P< 0.01$). n = numbers of cells measured for the comparison of nuclear eccentricity.

Author Manuscript Author Manuscript Author Manuscript Author Manuscript

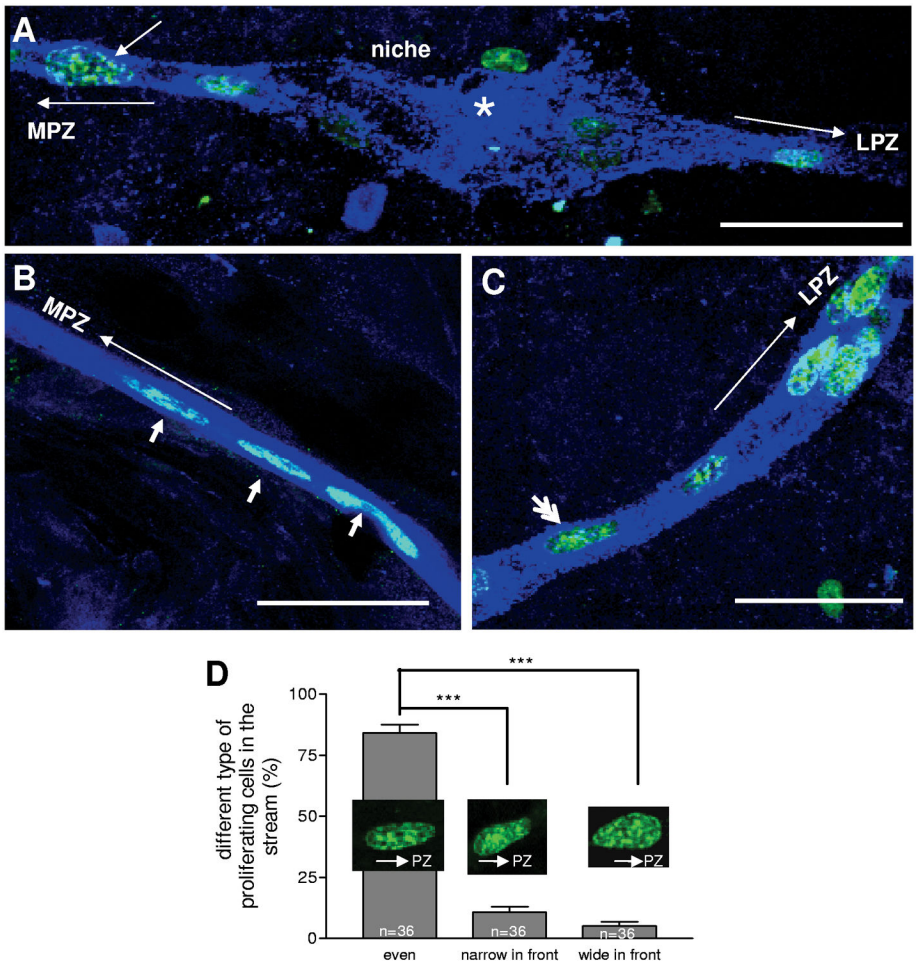

Figure 7.

Nuclear distortion of cells in the stream during migration. A-C: Examples of nuclei having the wider edge in the direction of migration (towards the proliferation zone) (short arrow in A), or the narrower edge towards proliferation zone (double arrowheads in C), or with symmetrical, elliptical nuclei (short arrows in B, labeled as ‘even’ in D). Long arrows indicate the direction of cell migration in the stream. The proportion of each group of cells with nuclear distortion were calculated in D. Data analyzed with one-way ANOVA. $P<0.0001$ in D. Significant differences between groups (Tukey multiple comparison) are marked with triple ($P<0.001$) asterisks. Scale bars are 50 μm in all images. A total 265 cells were characterized in 36 brain hemispheres (n) in D.

Author Manuscript Author Manuscript Author Manuscript Author Manuscript

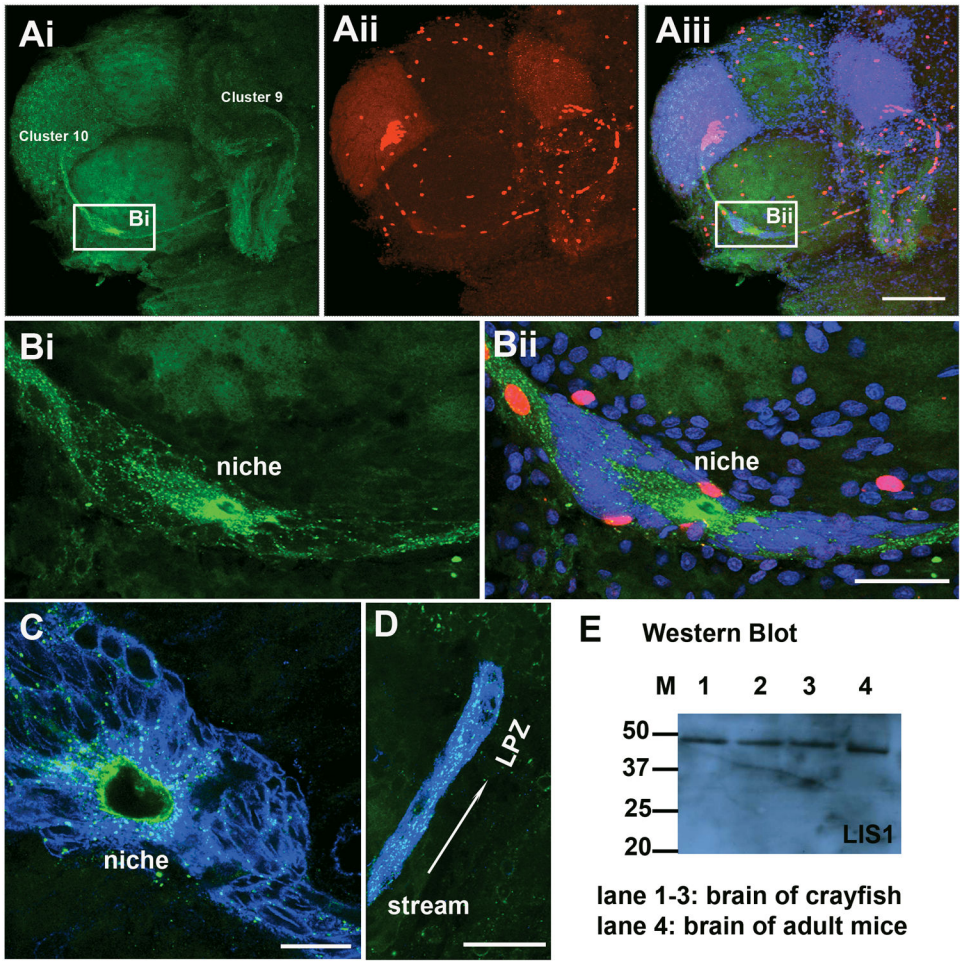

Figure 8.

Precursor cells express LIS1 protein. A-B: Whole mount brains were double-labeled for BrdU (red) and LIS1 (green) and counterstained with propidium iodide (blue), and optically sectioned with the confocal microscope. B shows higher magnification images of the niche, in the area indicated by the boxes in Ai and Aiii. C-D: double immunostaining of LIS1 (green) and glutamine synthetase (blue), showing punctate LIS1 staining in the cytoplasm of cells in the niche and stream. Scale bar = 200 μm in A; 50 μm in B and D; 20 μm in C. E: Western blot for LIS1 on protein preparations from *P. clarkii* brain (lane 1, 35 mm CL; lane 2, 16 mm CL; lane 3, 8 mm CL) and adult mouse brain (lane 4). M, protein molecular weight marker, number indicated as kDa.

Author Manuscript Author Manuscript Author Manuscript Author Manuscript

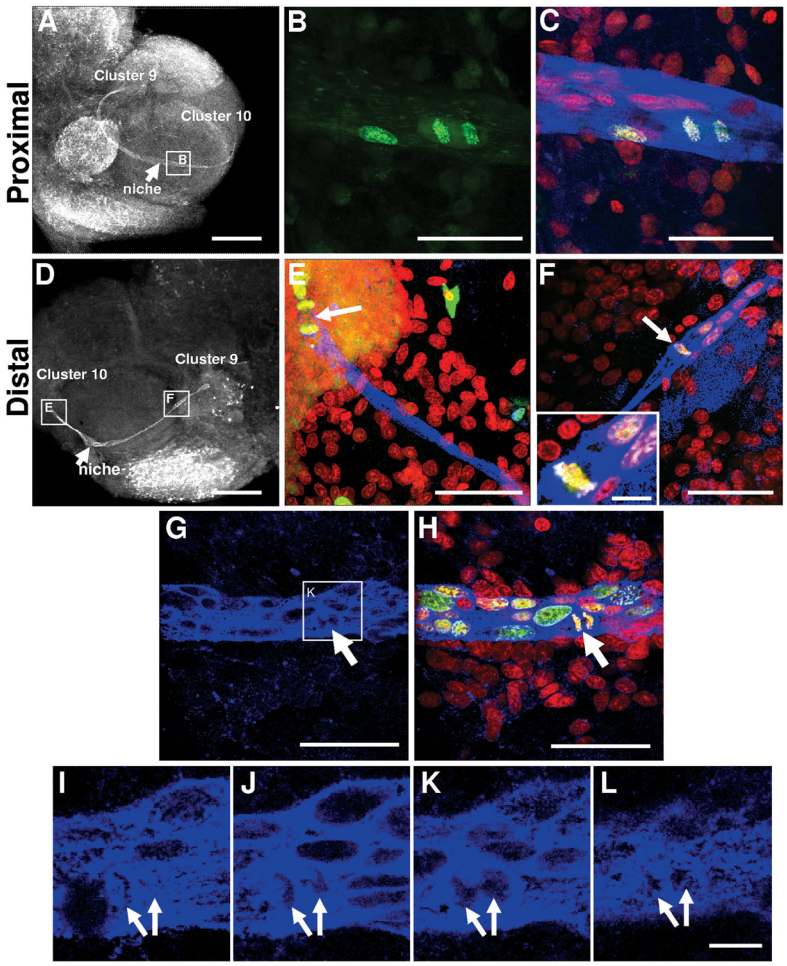

Figure 9.

Precursor cells divide at the ends of the stream proximal (A-C) and distal (D-F) to the niche, and generate daughters of similar size. Sections were double-labeled for BrdU (green) and glutamine synthetase (blue), and counterstained with propidium iodide (red). In A and D, glutamine synthetase staining was converted to black and white for better contrast. A-C: a dividing cell is in the proximal end of the stream, near the niche. A: lower magnification of a brain hemisphere with glutamine synthetase labeling. B-C: higher magnification view of boxed area in A. B, only BrdU-labeled channel is shown. C: merge of all three optical channels, showing labeling for BrdU, glutamine synthetase and propidium iodide. D: lower magnification of a brain hemisphere labeled for BrdU and glutamine synthetase, and marking regions shown at a higher magnification in E and F. E, a dividing cell (arrow) is at the distal end of the stream, close to Cluster 10. F: cell (arrow and inset) in metaphase is at the distal end of the stream close to Cluster 9. G-L show cells close to the niche undergoing cytokinesis (arrows). Sequential high magnification images of glutamine synthetase labeling I-L are extracted from the same stack of 1 μm images shown in G (boxed area) and H. Scale bars are 400 μm in A, 200 μm in D, 50 μm in B-C and E-H, 10 μm in I-L and inset in F.

Author Manuscript Author Manuscript Author Manuscript Author Manuscript

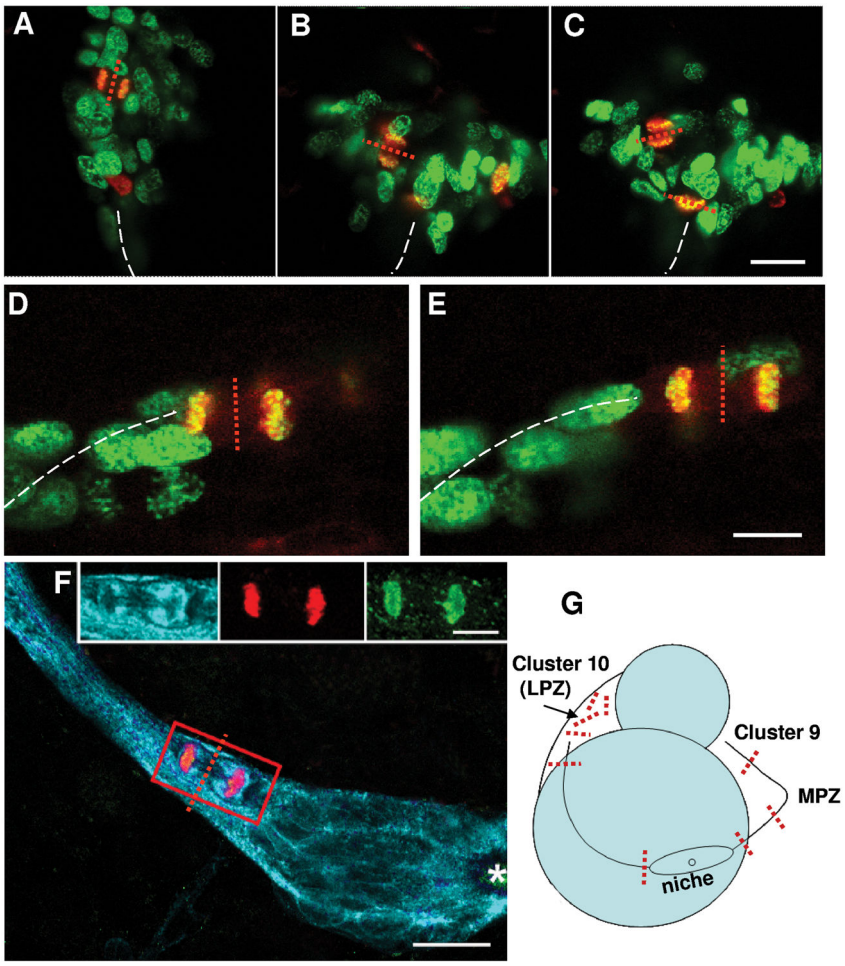

Figure 10.

Cleavage planes in the stream, LPZ and MPZ are compared. The cleavage planes are oriented perpendicular to the direction of migration in the streams and in Cluster 9, while cleavage planes in Cluster 10 are random. Crayfish (12 mm CL) were maintained in 2 mg/ml BrdU in artificial pond water for 8 hours prior to fixation, and double immunofluorescent labeling was done for BrdU (green) and phosphohistone-3 (red). A-C: M-phase cells in the LPZ (Cluster 10) double-labeled (yellow-orange) for both S- and M-phase markers. Metaphase and anaphase/telophase cells were found in the LPZ with condensed chromosomes aligned in the middle of the cells, or with separated chromatids. D-E: Anaphase/telophase cells in the middle of the stream between the MPZ and Cluster 9. White dashed lines indicate the path of the stream. The red dotted line represents the cleavage plane of each dividing cell. F: triple-labeled M-phase cell close to the niche immunolabeled with GS (cyan), phosphohistone-H3 (green) and BrdU (red). G: Summary of the cleavage planes of dividing cells observed in the stream and in the cell clusters. Representative cleavage planes are provided as red dotted lines in G. Scale bar is 20 μm in A-C and F, 10 μm in D-E and inset.

Author Manuscript Author Manuscript Author Manuscript Author Manuscript

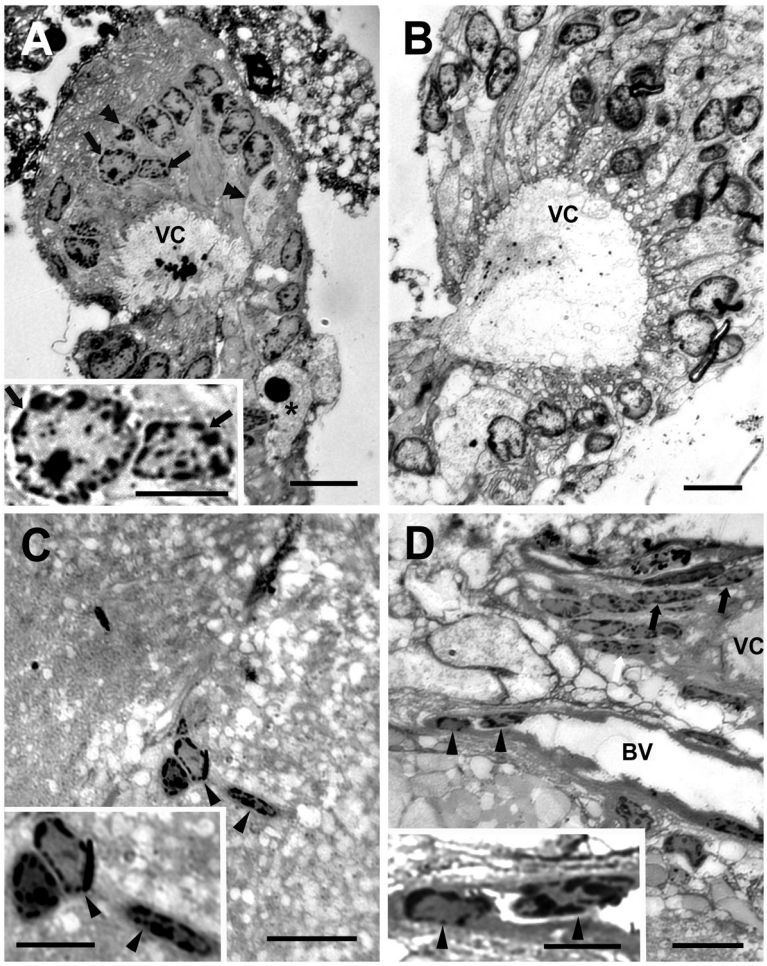

Figure 11.

Niche precursor cells and vascular cells compared in toluidine blue-stained semi-thin (0.5 μm) plastic sections of the niche and stream from intermediate-size crayfish (CL 20mm). A: Section through the vascular cavity (VC) and surrounding niche cells showing densely staining inclusions within the vascular cavity and finger-like cytoplasmic extensions into the cavity from the cells that border it. The most common cell type (Type I; arrows) contains a large nucleus with heterochromatin and euchromatin and one or more nucleoli. The cytoplasm of two of the niche cells (Type II; double arrowheads) bordering the cavity has stained less strongly than the others, and has a less prominent nucleus. A third distinctive cell type (Type III; asterisk) contains a darkly stained spherical nucleus and clear cytoplasmic vesicles, and has an amoeboid shape. B: Section through the vascular cavity (VC) and surrounding niche cells; dense granules were again seen in the cavity although these were smaller than in A and dispersed, rather than clustered, which may be related to the level of the section through the niche. Small finger-like cytoplasmic extensions are again present on the cells that border the cavity. In addition the cells bordering the cavity contain clear vacuoles, most of which are located close to their border with the vascular cavity. The nuclei of the cells contain the characteristic condensed chromatin and nucleoli, as in A. C: Cells in blood vessels deep within the neuropil of the accessory lobe exhibit a morphology very similar to those of the Type I niche cells that surround the vascular cavity. D: The

Author Manuscript Author Manuscript Author Manuscript Author Manuscript

blood vessel (BV) that lies beneath the niche contains cells (single arrowheads) with similar morphologies to the cells that surround the vascular cavity. Here the niche has been sectioned through a different plane than those shown in A and B and the niche cells appear thin and elongate. Only part of the vascular cavity (VC) is shown. Scale bars: 20 μm for A-D; 10 μm for insets.